Electronic Supplementary Material (ESI) for Journal of Materials Chemistry C.

Carboxyl group dominant carbon nanodot third-order nonlinear optical property

(Supporting Information)

Quantify the hydroxyl and carboxyl groups on the surface of the CNDs.

We carried out two sets of experiments to quantify the two kinds of oxygen-containing functional groups (carboxyl and hydroxyl groups). First, we performed base titration to determine the total quantity of both carboxyl and hydroxyl by a standard method. [15] The 0.05 mol•L^{-1} NaOH and 0.05 mol•L^{-1} HCl were used as titrant. NaOH (0.05 mol•L^{-1}, 2 mL) was added into a 50 mL beaker containing water soluble CNDs1 (1.84 mg•mL^{-1}, 10 mL) with stirring for 5 min. After that, the supernatant was back titrated by 0.05 mol•L^{-1} HCl to PH = 7. And it consumed 1.16 mL HCl. So the total quantity of both of carboxyl and hydroxyl could be confirmed through the following calculation formula:

n(carboxyl and hydroxyl) = (2 –0.98) mL × 0.05 mol•L^{-1} = 5.1 × 10^{-5} mol

So the total quantity of both of carboxyl and hydroxyl for 10 mL water soluble CNDs1 was 5.1 × 10^{-5} mol, and the total concentration for 1 g CNDs1 was 2.77 × 10^{-3} mol. In the later experiment, conductometric titration was carried out with a DDS-11A conductance titrator to quantify the relative content ratio of carboxyl versus hydroxyl. [16] CNDs1 (1.84 mg•mL^{-1}, 184.0 mg), 40 mL solvent (pyridine/acetone = 1/4), 1 mL ultrapure water and 1 mL absolute ethyl alcohol were added into a 50 mL 4-mouth flask. The above solution was stirred at 180 rpm at 25 ^{o}C for 15 min and 0.05 mol•L^{-1} KOH-isopropyl alcohol standard solution was used as the titrant. The conductivity-titrant amount curve was shown in Fig. 2A. Here, A and B were the equivalence points of carboxyl and hydroxyl of CNDs1, respectively. The contents of carboxyl and hydroxyl were gained through the following calculation formula:

n (carboxyl) = V_A × c = 4.86 × 10^{-3} L × 0.05 mol•L^{-1} = 2.43 × 10^{-4} mol

n (hydroxyl) = V_B × c = 18.86 × 10^{-3} L × 0.05 mol•L^{-1} = 9.43 × 10^{-4} mol

Therefore, based on the above experiment results, the relative content ratio of carboxyl/hydroxyl was about 1/3.88. Then, the relative content ratios of carboxyl/hydroxyl and carboxyl and hydroxyl content of the CNDs2, CNDs3, CNDs4 and low reduction CNDs (reduced by 0.1 M $NaBH_4$ solution, LR-CNDs) were also gained with the same method.

Calculation of oxygen content on the surface of CNDs.

Calculation of the oxygen-containing functional groups (-OH and -COOH) content in modified CNDs was done assuming one original single CND is a cube. The cube is seen as the original single CND, which consists of several carbon layers with hydroxyl or carboxyl groups on the surface of the cube. Herein, as an extreme case, we assume that the carbon atoms on the top and the bottom surface were not bond with other atoms while the carbon atoms exposed to the outside of the four sides of each layer were bond with oxygen atoms. Then, the maximum oxygen content of each carbon dot can be calculated. For example, a 5.9 nm sized cube CND, the carbon atoms exposed to the outside of the four sides of each layer = (47 × 2 + 27 × 2) = 148; The carbon atoms of

four sides exposed to the outside of the whole cube = 148 × 5.9/0.335 = 2607; All carbon atoms in the cube: 47 × 27 × 5.9/0.335 = 22350. The percentage of the carbon atoms of four sides exposed to the outside in total carbon atoms of the cube: 2607/22350 = 11.7%. Then, the oxygen content on surface of carbon dots can be calculated. The detailed quantification date of the four sizes CNDs are shown in Table S1.

The third-order nonlinear susceptibility coefficient $\chi_{zzz}^{(3)}$ of the CNDs samples was also calculated to understand the nature of the nonlinearity, which was given a rough estimate of the NLO properties by the following expression [29]:

$$\chi_{zzz}^{(3)} = \frac{C\alpha_0^3}{\sigma E_g^6 d^3}$$

where C is a constant, a_0 is the Bohr's radius, d is the average distance between neighboring carbon atoms, σ is the cross-sectional area per CND particle, and E_g, is the energy gap of the CNDs samples.

The Z-scan is a simple and popular experimental technique to measure the intensity dependent third-order nonlinear susceptibility of the materials. It allows the simultaneous measurement of both the nonlinear refractive index γ and the nonlinear absorption coefficient β. From these parameters, the real and the imaginary components of the third-order nonlinear susceptibility $\chi^{(3)}$ can be calculated using the following relations [27]:

$$T(Z) = \frac{\alpha_0}{\sqrt{\pi}\beta I_i(Z)(1 - e^{-\alpha_0 L})} \int_{-\infty}^{\infty} ln\left[1 + \beta I_i(Z)\frac{1 - e^{-\alpha_0 L}}{\alpha_0} e^{-\tau^2}\right] d\tau \quad (1)$$

$$\gamma = \frac{\Delta T_{p-v}\lambda}{0.812\pi I_0 (1 - S)^{0.25} L_{eff}} \quad (2)$$

$$\chi_{Re}^{(3)}(esu) = \frac{cn_0^2\gamma}{120\pi^2} \quad (3)$$

$$\chi_{Im}^{(3)}(esu) = \frac{n_0^2 c^2 \beta}{240\pi^2 \omega} \quad (4)$$

$$\chi^{(3)} = \left[\left(\chi_{Im}^{(3)}\right)^2 + \left(\chi_{Re}^{(3)}\right)^2\right]^{\frac{1}{2}} \quad (5)$$

where L_{eff} is the effective sample thickness, α_0 is the linear absorption coefficient at the excitation wavelength λ, L is the sample length, I_0 is the laser peak irradiance on the focal plane, z_0 is the Rayleigh length, z is the position of the sample, ΔT_{p-v} is the difference between the peak and the valley of the normalized transmittance, and S is the linear transmittance of the aperture, defined as $S = 1 - \exp(-2r_a^2/w_a^2)$, with r_a being the radius of the aperture and w_a being the beam radius at the aperture.

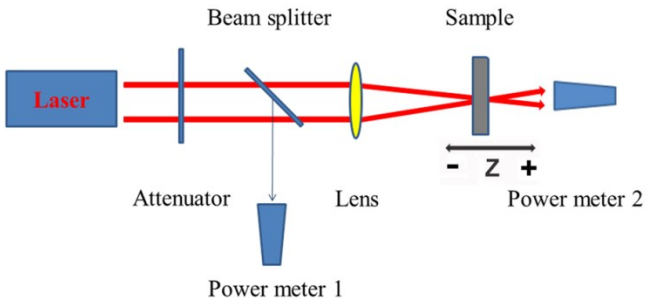

Fig. S1 Experimental arrangement for Z-scan measurement.

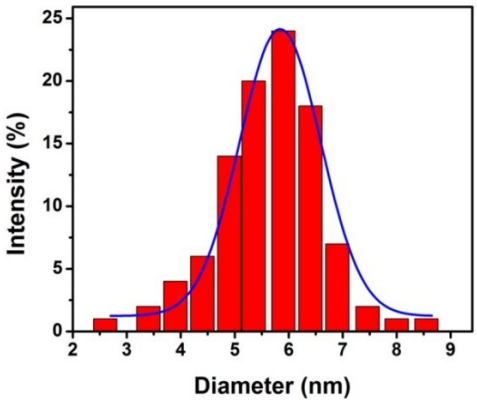

Fig. S2 (A) Partical-size histogram of CNDs1.

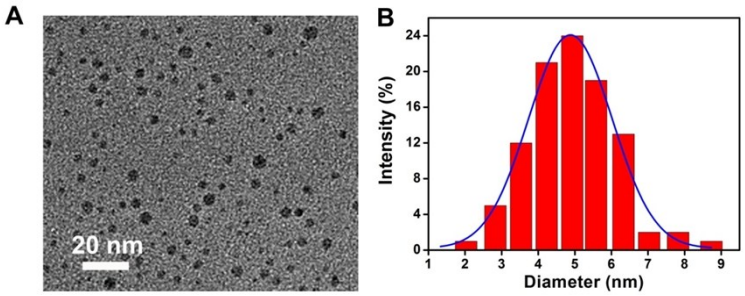

Fig. S3 (A) TEM image and (B) partical-size histogram of CNDs2.

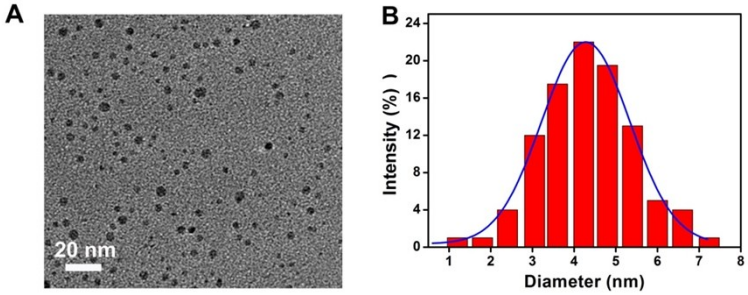

Fig. S4 (A) TEM image and (B) partical-size histogram of CNDs3.

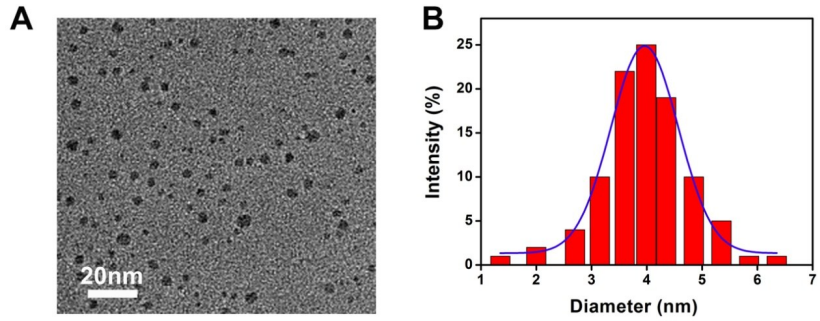

Fig. S5 (A) TEM image and (B) partical-size histogram of CNDs4.

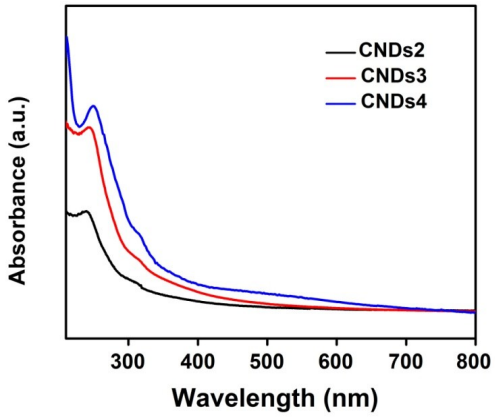

Fig. S6 UV-vis absorption spectra of CNDs2 (black line), CNDs3 (red line) and CNDs4 (blue line).

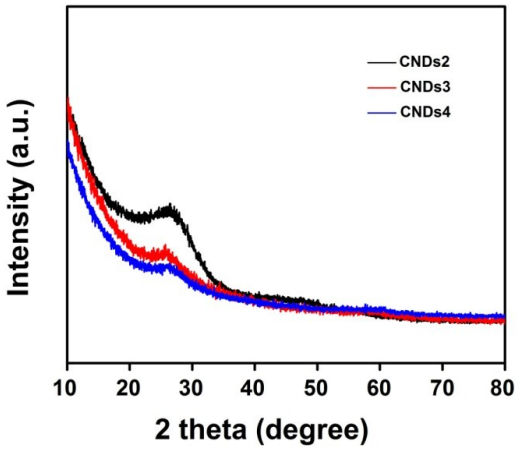

Fig. S7 XRD patterns of CNDs2 (black line), CNDs3 (red line) and CNDs4 (blue line).

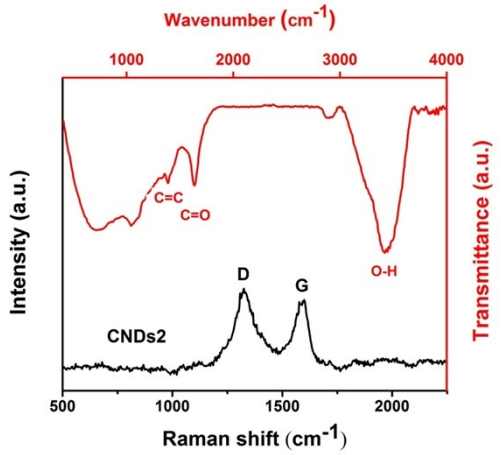

Fig. S8 Raman (black line) and FTIR (red line) spectra of CNDs2.

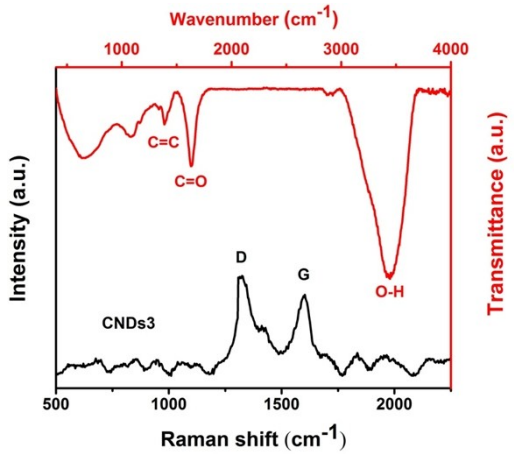

Fig. S9 Raman (black line) and FTIR (red line) spectra of CNDs3.

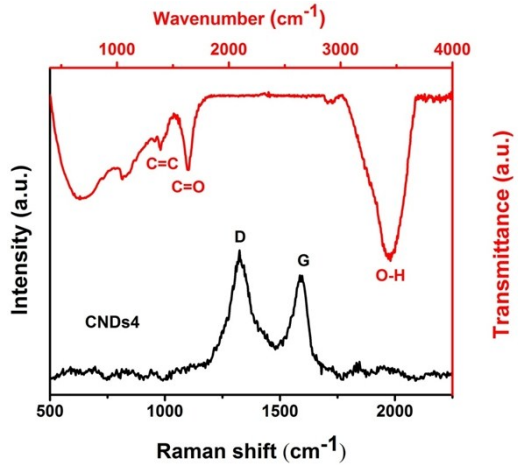

Fig. S10 Raman (black line) and FTIR (red line) spectra of CNDs4.

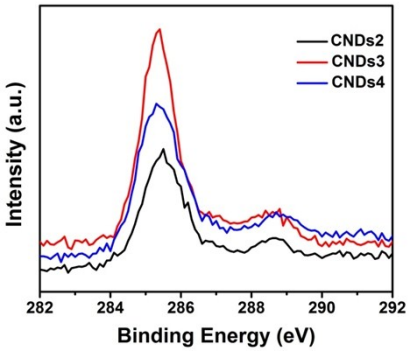

Fig. S11 The high-resolution C 1s XPS spectra of CNDs2 (black line), CNDs3 (red line) and CNDs4 (blue line).

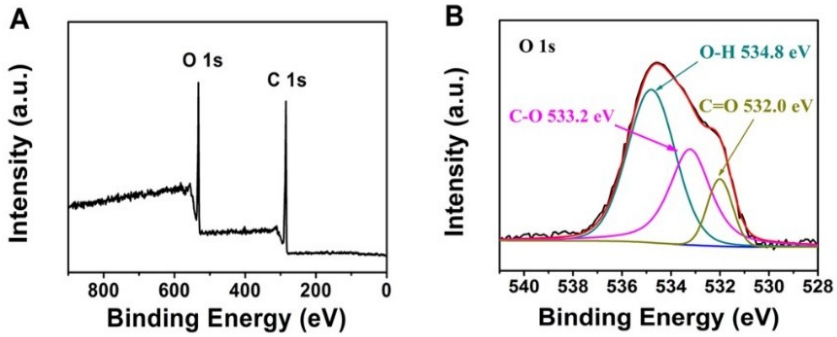

Fig. S12 The XPS full scan (A) and high-resolution O 1s (B) spectra of CNDs1.

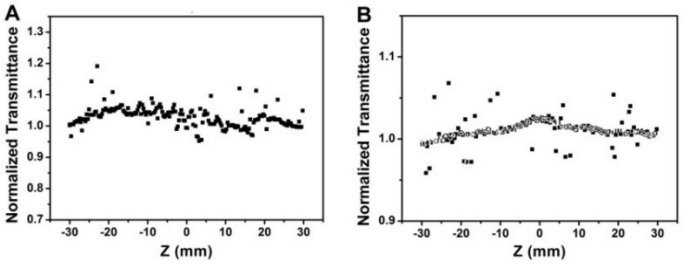

Fig. S13 (A) Close aperture and (B) open aperture Z-scan results of H_2O under 532 nm laser excitation.

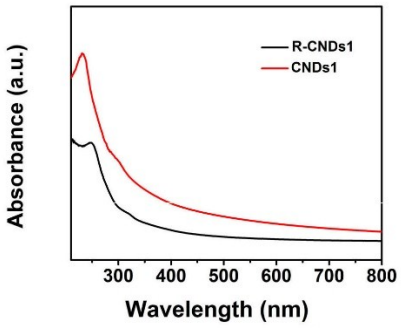

Fig. S14 UV-vis absorption spectra of CNDs1 (red line) and LR-CNDs1$_A$ (black line). The absorption shoulder at about 231 nm of LR-CNDs1$_A$ samples has 18 nm blue shift after $NaBH_4$ reduction.

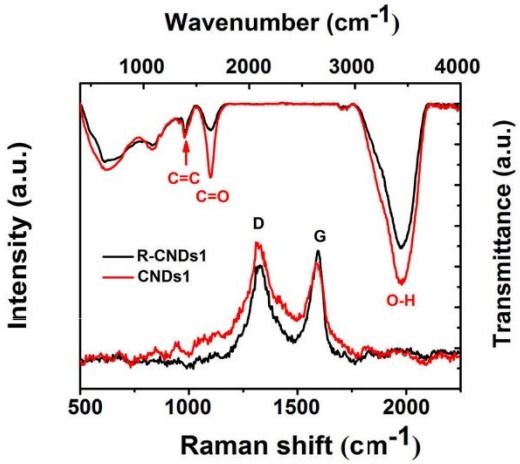

Fig. S15 Raman and FTIR spectra of CNDs1 (red line) and LR-CNDs1$_A$ (black line). As shown, after reacting with $NaBH_4$ solution, the carbonyl group of LR-CNDs1$_A$ decreases significantly, while other kinds of functional groups changed little. The intensity ratio of the D and G band (I_D/I_G) of LR-CNDs1$_A$ (1.46) is obviously higher than that of CNDs1 (1.18) which indicates the formation of more defective carbonaceous structures after the reduction reaction with $NaBH_4$ solution.

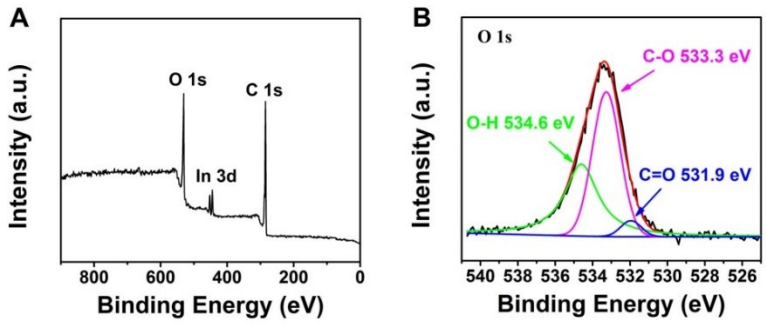

Fig. S16 The XPS full scan (A) and high-resolution O 1s (B) spectra of LR-CNDs1$_A$.

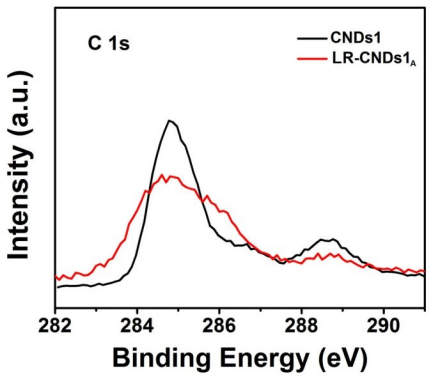

Fig. S17 The XPS high-resolution C 1s spectra of CNDs1 (black line) and LR-CNDs1$_A$ (red line).

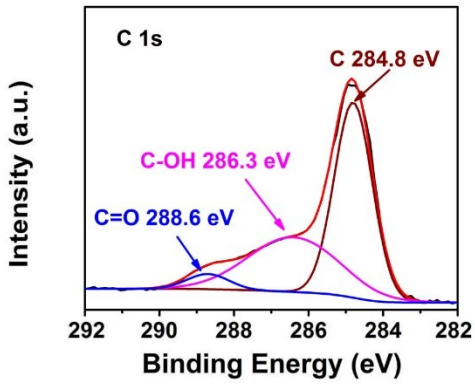

Fig. S18 The high-resolution C 1s XPS spectrum of LR-CNDs1$_A$. It can be divided into three component peaks located at about 284.8, 286.3 and 288.6 eV, which confirms the presence of C-C, C-OH and C=O bonds. Compared with the high-resolution C 1s XPS spectrum of CNDs1 (Fig. 1E), the C=O content of LR-CNDs1$_A$ decreases significantly.

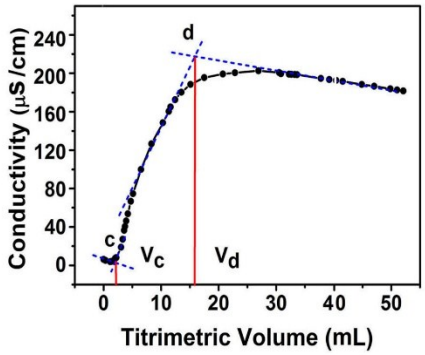

Fig. S19 The conductivity-titrant amount curve of LR-CNDs1$_A$. The relative content of carboxyl versus hydroxyl of LR-CNDs1$_A$ is about 1:7.81 (Vc:Vd), which demonstrates carboxyl content decreases obviously after $NaBH_4$ reduction.

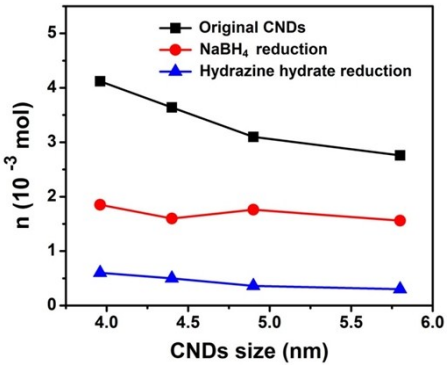

Fig. S20 Size dependence of the molar content of oxygen-containing functional groups of 1 g original CNDs and CNDs reduced by $NaBH_4$ solution (0.1M) and hydrazine hydrate solution (0.1M), respectively.

Table S1 The experimental and calculated results of functional groups on the surface of CNDs.

sample	size/nm	$\eta_{edge\ carbon}$[a]/%	n_{cal}[b] (COOH & OH)/10^{-3} mol	n_{exp}[c] (COOH & OH)/10^{-3} mol	$Ratio_{exp}$[d] (COOH/OH)	
					CNDs	[e]LR-CNDs$_A$
1	5.8	11.7	8.4	2.77	1 : 3.88	1 : 7.81
2	4.9	13.7	9.6	3.1	1 : 4	1 : 8.26
3	4.4	15.1	10.5	3.64	1 : 3.92	1 : 8.06
4	3.96	16.8	11.4	4.12	1 : 4	1 : 8.2

[a] The percentage of edge carbon atoms in total carbon atoms of the cube.

[b, c] Calculated and experimental amount of substance of -COOH and -OH for 1g samples, respectively.

[d] The molar ratio of -COOH to -OH for 1g sample obtain from the experiment.

[e] Low reduction CNDs (LR-CNDs$_A$, reduced by 0.1 M $NaBH_4$ solution).

Table S2. The Third-Order Nonlinear Optical Parameters of the CNDs at 532 nm laser excitation

Sample	γ (10^{-17} m^2/W)	β (10^{-10} m/W)	$\chi^{(3)}$ (10^{-11} esu)	$\chi^{(3)}$/C (10^{-11} esu·mL·mg^{-1})
CNDs1	-5.3	0.8	2.394	1.301
CNDs2	-5.3	0.8	2.390	1.127
CNDs3	-4.5	2.0	2.029	0.837
CNDs4	-1.0	4.1	0.943	0.332